

Supplementary Materials: DIDO: Deep Inertial Quadrotor Dynamical Odometry

Kunyi Zhang^{1,2} - kunyizhang@zju.edu.cn
Chenxing Jiang^{1,2} - chenxingjiang@zju.edu.cn
Jinghang Li² - jhanglee.ro@gmail.com
Sheng Yang³ - richeng.ys@alibaba-inc.com
Teng Ma³ - damon.mt@alibaba-inc.com
Chao Xu^{1,2} - chaoxu@zju.edu.cn
Fei Gao^{1,2} - fgaoaa@zju.edu.cn

CONTENTS

Acknowledgement	1
I IMU Kinematics and Quadrotor Dynamics	2
I-A IMU Kinematics	2
I-B Quadrotor Dynamics	2
II Two-Stage EKF for Inertial Dynamical Fusion	3
II-A Rotation Stage	3
II-A.1 State	3
II-A.2 Process Model	3
II-A.3 Measurement Model	3
II-A.4 Extended Kalman Filter	3
II-B Translation Stage	4
II-B.1 State	4
II-B.2 Process Model	4
II-B.3 Measurement Models	5
II-B.4 Discrete Extended Kalman Filter	6
III One-Stage EKF for Inertial Dynamical Fusion	6
III-A State	6
III-B Process Model	6
III-C Measurement Model	7
III-C.1 gravity alignment measurements	7
III-C.2 dynamics constraint measurements	7
III-C.3 network velocity measurements	8
III-C.4 network displacement measurements	8
III-D Discrete Extended Kalman Filter	9
IV Observability Analysis	9

¹State Key Laboratory of Industrial Control Technology, Institute of Cyber-Systems and Control, Zhejiang University, Hangzhou 310027, China.

²Huzhou Institute, Zhejiang University, Huzhou 313000, China.

³Alibaba DAMO Academy Autonomous Driving Lab, Hangzhou 311121, China.

I. IMU KINEMATICS AND QUADROTOR DYNAMICS

A. IMU Kinematics

IMU measurements include the gyroscope $\tilde{\boldsymbol{\omega}}$ and non-gravitational acceleration $\tilde{\boldsymbol{a}}$, which are measured in the IMU frame (the \mathcal{I} frame) and given by:

$$\begin{aligned}\mathcal{I}\tilde{\boldsymbol{\omega}} &= \mathcal{I}\boldsymbol{\omega} + \mathcal{I}\boldsymbol{b}_{\boldsymbol{\omega}} + \boldsymbol{n}_{\boldsymbol{\omega}}, \\ \mathcal{I}\tilde{\boldsymbol{a}} &= \mathcal{I}\boldsymbol{a} + \mathcal{I}\boldsymbol{b}_{\boldsymbol{a}} + \mathcal{I}\mathbf{R}^{\mathcal{G}}\mathbf{g} + \boldsymbol{n}_{\boldsymbol{a}},\end{aligned}\quad (1)$$

where $\mathcal{I}\boldsymbol{\omega}$ and $\mathcal{I}\boldsymbol{a}$ are the true angular velocity and acceleration, $\mathcal{G}\mathbf{g} = [0, 0, 9.8]$ is the gravity vector in the gravity-aligned frame (the \mathcal{G} frame), $\mathcal{I}\mathbf{R}$ is the rotation matrix from the \mathcal{I} frame to the \mathcal{G} frame, $\boldsymbol{n}_{\boldsymbol{\omega}}$ and $\boldsymbol{n}_{\boldsymbol{a}}$ are the additive Gaussian white noise in gyroscope and acceleration measurements, $\boldsymbol{b}_{\boldsymbol{\omega}}$ and $\boldsymbol{b}_{\boldsymbol{a}}$ are the bias of IMU modeled as random walk:

$$\begin{aligned}\boldsymbol{n}_{\boldsymbol{\omega}} &\sim \mathcal{N}(0, \boldsymbol{\Sigma}_{\boldsymbol{\omega}}^2), \quad \dot{\boldsymbol{b}}_{\boldsymbol{\omega}} \sim \mathcal{N}(0, \boldsymbol{\Sigma}_{\dot{\boldsymbol{b}}_{\boldsymbol{\omega}}}^2), \\ \boldsymbol{n}_{\boldsymbol{a}} &\sim \mathcal{N}(0, \boldsymbol{\Sigma}_{\boldsymbol{a}}^2), \quad \dot{\boldsymbol{b}}_{\boldsymbol{a}} \sim \mathcal{N}(0, \boldsymbol{\Sigma}_{\dot{\boldsymbol{b}}_{\boldsymbol{a}}}^2).\end{aligned}\quad (2)$$

B. Quadrotor Dynamics

Because the propagation of kinematic states are driven by multiple propulsion units in a quadrotor system, we model the Newtonian dynamics according to [1]. The total driving force of a quadrotor in the body frame (the \mathcal{B} frame) is the sum of the thrust ${}^{\mathcal{B}}\mathbf{F}_t$ and drag force ${}^{\mathcal{B}}\mathbf{F}_d$ generated by each propulsion unit as follow:

$${}^{\mathcal{B}}\mathbf{F} = \sum_{i=1}^4 ({}^{\mathcal{B}}\mathbf{F}_{t_i} - {}^{\mathcal{B}}\mathbf{F}_{d_i}) = \sum_{i=1}^4 (\tau u_i^2 \mathbf{e}_3 - u_i D \mathcal{B}\mathbf{v}_i), \quad (3)$$

where τ is the thrust coefficient for the propellers, $D = \text{diag}(d_x, d_y, d_z)$ is the matrix of effective linear drag coefficients, $\mathbf{e}_3 = [0, 0, 1]^{\top}$ is the z axis in any frame, and u_i and ${}^{\mathcal{B}}\mathbf{v}_i$ are the rotation speed and velocity of the i -th rotor, respectively. Actually, the velocity of each rotor is:

$${}^{\mathcal{B}}\mathbf{v}_i = {}^{\mathcal{B}}\mathbf{v} + {}^{\mathcal{B}}\boldsymbol{\omega} \times {}^{\mathcal{B}}\mathbf{r}_i^{\mathcal{B}}, \quad (4)$$

where ${}^{\mathcal{B}}\mathbf{v}$ and ${}^{\mathcal{B}}\boldsymbol{\omega}$ are the linear and angular velocity of the quadrotor's center of mass (*CoM*), ${}^{\mathcal{B}}\mathbf{r}_i^{\mathcal{B}}$ is the position of the i -th rotor relative to the *CoM*. To simplify the calculation, we ignore the velocity discrepancy of different rotors and express it as:

$${}^{\mathcal{B}}\mathbf{v}_i \approx {}^{\mathcal{B}}\mathbf{v}. \quad (5)$$

The input notations are abbreviated as:

$$U_{ss} = \sum_{i=1}^4 u_i^2, \quad U_s = \sum_{i=1}^4 u_i, \quad (6)$$

so we can obtain the Newtonian equation in the \mathcal{G} frame:

$$m \frac{d}{dt} ({}^{\mathcal{G}}\mathbf{v}) = {}^{\mathcal{B}}\mathbf{R} (\tau U_{ss} \mathbf{e}_3 - U_s D {}^{\mathcal{B}}\mathbf{R}^{\mathcal{G}} {}^{\mathcal{G}}\mathbf{v}) - m {}^{\mathcal{G}}\mathbf{g}. \quad (7)$$

II. TWO-STAGE EKF FOR INERTIAL DYNAMICAL FUSION

A. Rotation Stage

1) *State*: In the rotation stage, the rotation of the \mathcal{I} frame in the \mathcal{G} frame is taken as state:

$$\mathbf{x} = {}_{\mathcal{I}}^{\mathcal{G}}\mathbf{q}. \quad (8)$$

2) *Process Model*: The rotational equation is given:

$${}_{\mathcal{I}}^{\mathcal{G}}\dot{\mathbf{q}} = \frac{1}{2} {}_{\mathcal{I}}^{\mathcal{G}}\mathbf{q} \otimes {}^{\mathcal{I}}\boldsymbol{\omega} = \frac{1}{2} {}_{\mathcal{I}}^{\mathcal{G}}\mathbf{q} \otimes ({}^{\mathcal{I}}\hat{\boldsymbol{\omega}} + \mathbf{n}_{\boldsymbol{\omega}}), \quad (9)$$

where ${}^{\mathcal{I}}\hat{\boldsymbol{\omega}}$ is the gyroscope outputs of *De-Bias Net*.

The above differential equation is discretized as follows:

$$\begin{aligned} \mathbf{x}_{k+1} &= \mathbf{F}(\mathbf{x}_k, \mathbf{u}_k, \mathbf{n}_k) \\ &= \mathbf{F}_x \mathbf{x}_k + \mathbf{F}_n \mathbf{n}_k, \end{aligned} \quad (10)$$

where,

$$\begin{aligned} \mathbf{F}_x &= \frac{\partial \mathbf{F}}{\partial \mathbf{x}_k} = \mathbf{I}_4 + \frac{\Delta t}{2} \begin{bmatrix} 0 & -{}^{\mathcal{I}}\hat{\boldsymbol{\omega}}^\top \\ {}^{\mathcal{I}}\hat{\boldsymbol{\omega}} & [{}^{\mathcal{I}}\hat{\boldsymbol{\omega}}]_\times \end{bmatrix}, \\ \mathbf{F}_n &= \frac{\partial \mathbf{F}}{\partial \mathbf{n}_{\boldsymbol{\omega}}} = \frac{\Delta t}{2} \begin{bmatrix} -q_x & -q_y & -q_z \\ q_w & -q_z & q_y \\ q_z & q_w & -q_x \\ -q_y & q_x & q_w \end{bmatrix} = \frac{\Delta t}{2} \begin{bmatrix} -\mathbf{q}_v \\ q_w \mathbf{I}_3 + [\mathbf{q}_v]_\times \end{bmatrix}. \end{aligned} \quad (11)$$

Specifically, $\mathbf{q} = [q_w, q_x, q_y, q_z]^\top = [q_w, \mathbf{q}_v^\top]^\top$.

3) *Measurement Model*: The attitude controllers of most flying robots rely on the complementary filters [2, 3] to obtain attitude observations. Similarly, we consider the gravity alignment constraint to obtain the tilt observation:

$${}^{\mathcal{I}}\hat{\mathbf{a}} \approx {}_{\mathcal{I}}^{\mathcal{G}}\mathbf{R}^{\top \mathcal{G}}\mathbf{g} + \mathbf{n}_a. \quad (12)$$

The above observation equation is approximated as:

$$\mathbf{z}_k = \mathbf{H}(\mathbf{x}_k) = \mathbf{H}_x \mathbf{x}_k, \quad (13)$$

where,

$$\mathbf{H}_x = 2 \begin{bmatrix} \mathbf{e}_3 \times \mathbf{q}_v & [\mathbf{e}_3 \times \mathbf{q}_v + q_w \mathbf{e}_3]_\times + (\mathbf{q}_v \cdot \mathbf{e}_3) \mathbf{I}_3 - \mathbf{e}_3 \mathbf{q}_v^\top \end{bmatrix}. \quad (14)$$

4) *Extended Kalman Filter*:

$$\begin{aligned} \mathbf{x}_{k+1|k} &= \mathbf{F}(\mathbf{x}_{k|k}, \mathbf{u}_k), \\ \mathbf{P}_{k+1|k} &= \mathbf{F}_x \mathbf{P}_{k|k} \mathbf{F}_x^T + \mathbf{F}_u \mathbf{Q}_k \mathbf{F}_u^T, \\ \mathbf{K}_{k+1} &= \mathbf{P}_{k+1|k} \mathbf{H}_x^T (\mathbf{H}_x \mathbf{P}_{k+1|k} \mathbf{H}_x^T + \mathbf{R}_{k+1})^{-1}, \\ \mathbf{x}_{k+1|k+1} &= \mathbf{x}_{k+1|k} \oplus (\mathbf{K}_{k+1} (\mathbf{z}_{k+1} - \mathbf{H}(\mathbf{x}_{k+1|k}))), \\ \mathbf{P}_{k+1|k+1} &= (\mathbf{I} - \mathbf{K}_{k+1} \mathbf{H}_x) \mathbf{P}_{k+1|k}, \end{aligned} \quad (15)$$

where,

$$\mathbf{Q} = \Sigma_{\boldsymbol{\omega}}^2, \quad \mathbf{R} = \Sigma_a^2. \quad (16)$$

B. Translation Stage

1) *State*: The state of the second stage is defined as:

$$\mathbf{x} = (^{\mathcal{G}}\mathbf{p}_{\mathcal{B}}^{\mathcal{G}}, ^{\mathcal{G}}\mathbf{v}_{\mathcal{B}}^{\mathcal{G}}, \tau, \mathbf{d}, {}^{\mathcal{I}}_{\mathcal{B}}\mathbf{q}, {}^{\mathcal{I}}\mathbf{t}_{\mathcal{B}}^{\mathcal{I}}), \quad (17)$$

where ${}^{\mathcal{G}}\mathbf{p}_{\mathcal{B}}^{\mathcal{G}}$ and ${}^{\mathcal{G}}\mathbf{v}_{\mathcal{B}}^{\mathcal{G}}$ are respectively the velocity and position of the quadrotor body \mathcal{B} frame expressed in the \mathcal{G} frame, τ is the thrust coefficient, \mathbf{d} is the drag vector of (d_x, d_y, d_z) , and $({}^{\mathcal{I}}_{\mathcal{B}}\mathbf{q}, {}^{\mathcal{I}}\mathbf{t}_{\mathcal{B}}^{\mathcal{I}})$ is the extrinsic parameter between the \mathcal{B} and the \mathcal{I} frame.

2) *Process Model*: We regard the quadrotor dynamics as the input, and express the complete process model as follows:

$$\begin{aligned} {}^{\mathcal{G}}\dot{\mathbf{p}}_{\mathcal{B}}^{\mathcal{G}} &= {}^{\mathcal{G}}\mathbf{v}_{\mathcal{B}}^{\mathcal{G}}, \\ {}^{\mathcal{G}}\dot{\mathbf{v}}_{\mathcal{B}}^{\mathcal{G}} &= \frac{1}{m} {}^{\mathcal{G}}_{\mathcal{B}}\mathbf{R} \left(\tau U_{ss} \mathbf{e}_3 - U_s D_{\mathcal{B}}^{\mathcal{G}} \mathbf{R}^{\top} {}^{\mathcal{G}}\mathbf{v}_{\mathcal{B}}^{\mathcal{G}} + \hat{\mathbf{f}}_{res} + \mathbf{n}_f \right) - {}^{\mathcal{G}}\mathbf{g}, \\ \dot{\tau} &= 0, \\ \dot{\mathbf{d}} &= 0, \\ {}^{\mathcal{I}}_{\mathcal{B}}\dot{\mathbf{q}} &= 0, \\ {}^{\mathcal{I}}\dot{\mathbf{t}}_{\mathcal{B}}^{\mathcal{I}} &= 0, \end{aligned} \quad (18)$$

where ${}^{\mathcal{G}}_{\mathcal{B}}\mathbf{R} = {}^{\mathcal{I}}_{\mathcal{B}}\mathbf{R}^{\top} {}^{\mathcal{I}}\mathbf{R}$ is the rotation from the quadrotor body \mathcal{B} frame to the \mathcal{G} frame, and $\mathbf{n}_f \sim \mathcal{N}(0, \hat{\Sigma}_f^2)$.

The above differential equation is discretized as follows:

$$\begin{aligned} \mathbf{x}_{k+1} &= \mathbf{F}(\mathbf{x}_k, \mathbf{u}_k, \mathbf{n}_k) \\ &= \mathbf{F}_x \mathbf{x}_k + \mathbf{F}_n \mathbf{n}_k, \end{aligned} \quad (19)$$

where,

$$\begin{aligned} \mathbf{F}_x &= \begin{bmatrix} \mathbf{I}_3 & \frac{\partial \mathbf{p}_{k+1}}{\partial \mathbf{v}_k} & \mathbf{0}_{31} & \mathbf{0}_3 & \mathbf{0}_3 & \mathbf{0}_3 \\ \mathbf{0}_3 & \frac{\partial \mathbf{v}_{k+1}}{\partial \mathbf{v}_k} & \frac{\partial \mathbf{v}_{k+1}}{\partial \tau} & \frac{\partial \mathbf{v}_{k+1}}{\partial \mathbf{d}} & \frac{\partial \mathbf{v}_{k+1}}{\partial {}^{\mathcal{I}}_{\mathcal{B}}\boldsymbol{\theta}} & \mathbf{0}_3 \\ \mathbf{0}_{13} & \mathbf{0}_{13} & 1 & \mathbf{0}_{13} & \mathbf{0}_{13} & \mathbf{0}_{13} \\ \mathbf{0}_3 & \mathbf{0}_3 & \mathbf{0}_{31} & \mathbf{I}_3 & \mathbf{0}_3 & \mathbf{0}_3 \\ \mathbf{0}_3 & \mathbf{0}_3 & \mathbf{0}_{31} & \mathbf{0}_3 & \mathbf{I}_3 & \mathbf{0}_3 \\ \mathbf{0}_3 & \mathbf{0}_3 & \mathbf{0}_{31} & \mathbf{0}_3 & \mathbf{0}_3 & \mathbf{I}_3 \end{bmatrix}, \\ \mathbf{F}_n &= \left[\mathbf{0}_3 \quad \frac{\partial \mathbf{v}_{k+1}}{\partial \mathbf{n}_f} \quad \mathbf{0}_{31} \quad \mathbf{0}_3 \quad \mathbf{0}_3 \quad \mathbf{0}_3 \right]^{\top}. \end{aligned} \quad (20)$$

Specifically,

$$\begin{aligned} \frac{\partial \mathbf{p}_{k+1}}{\partial \mathbf{v}_k} &= \mathbf{I}_3 \Delta t, \\ \frac{\partial \mathbf{v}_{k+1}}{\partial \mathbf{v}_k} &= \mathbf{I} - \frac{U_s \Delta t}{m} {}^{\mathcal{G}}_{\mathcal{B}}\mathbf{R} D_{\mathcal{B}}^{\mathcal{G}} \mathbf{R}^{\top}, \\ \frac{\partial \mathbf{v}_{k+1}}{\partial \tau} &= \frac{U_{ss} \Delta t}{m} {}^{\mathcal{G}}_{\mathcal{B}}\mathbf{r}_3, \\ \frac{\partial \mathbf{v}_{k+1}}{\partial \mathbf{d}} &= -\frac{\Delta t}{m} [{}^{\mathcal{G}}_{\mathcal{B}}\mathbf{r}_1 {}^{\mathcal{G}}_{\mathcal{B}}\mathbf{r}_1^{\top} {}^{\mathcal{G}}\mathbf{v}_{\mathcal{B}}^{\mathcal{G}} \quad {}^{\mathcal{G}}_{\mathcal{B}}\mathbf{r}_2 {}^{\mathcal{G}}_{\mathcal{B}}\mathbf{r}_2^{\top} {}^{\mathcal{G}}\mathbf{v}_{\mathcal{B}}^{\mathcal{G}} \quad {}^{\mathcal{G}}_{\mathcal{B}}\mathbf{r}_3 {}^{\mathcal{G}}_{\mathcal{B}}\mathbf{r}_3^{\top} {}^{\mathcal{G}}\mathbf{v}_{\mathcal{B}}^{\mathcal{G}}], \\ \frac{\partial \mathbf{v}_{k+1}}{\partial {}^{\mathcal{I}}_{\mathcal{B}}\boldsymbol{\theta}} &= \frac{\Delta t}{m} {}^{\mathcal{G}}_{\mathcal{B}}\mathbf{R} \left(-\tau U_{ss} [\mathbf{e}_3]_{\times} + U_s \left([D_{\mathcal{B}}^{\mathcal{G}} \mathbf{R}^{\top} {}^{\mathcal{G}}\mathbf{v}_{\mathcal{B}}^{\mathcal{G}}]_{\times} - D [{}^{\mathcal{G}}_{\mathcal{B}}\mathbf{R}^{\top} {}^{\mathcal{G}}\mathbf{v}_{\mathcal{B}}^{\mathcal{G}}]_{\times} \right) - [\hat{\mathbf{f}}_{res}]_{\times} \right), \\ \frac{\partial \mathbf{v}_{k+1}}{\partial \mathbf{n}_f} &= \frac{1}{m} {}^{\mathcal{G}}_{\mathcal{B}}\mathbf{R} \Delta t, \end{aligned} \quad (21)$$

and $\mathbf{r}_i = \mathbf{R} \mathbf{e}_i$.

3) *Measurement Models*: There are three measurements corresponding to the translation stage: the IMU acceleration, the network velocity and the network displacement measurements.

a) *dynamics constraint measurements*: The dynamics constraint measurements are expressed as:

$$\begin{aligned} {}^{\mathcal{I}}\hat{\mathbf{a}} &= \mathbf{H}_d(\mathbf{x}, \mathbf{n}_a) \\ &= \frac{1}{m} {}^{\mathcal{I}}\mathbf{R} \left(\tau U_{ss} \mathbf{e}_3 - U_s D_{\mathcal{B}}^{\mathcal{G}} \mathbf{R}^{\top \mathcal{G}} \mathbf{v}_{\mathcal{B}}^{\mathcal{G}} + \hat{\mathbf{f}}_{res} \right) + {}^{\mathcal{I}}\hat{\boldsymbol{\omega}} \times ({}^{\mathcal{I}}\hat{\boldsymbol{\omega}} \times {}^{\mathcal{I}}\mathbf{t}_{\mathcal{B}}^{\mathcal{I}}) + {}^{\mathcal{I}}\hat{\boldsymbol{\alpha}} \times {}^{\mathcal{I}}\mathbf{t}_{\mathcal{B}}^{\mathcal{I}} + \mathbf{n}_a, \end{aligned} \quad (22)$$

whose jacobian can be given as:

$$\frac{\partial \mathbf{H}_d}{\partial \mathbf{x}_k} = \begin{bmatrix} \mathbf{0}_3 & \frac{\partial \mathbf{H}_d}{\partial \mathbf{v}_k} & \frac{\partial \mathbf{H}_d}{\partial \tau} & \frac{\partial \mathbf{H}_d}{\partial \mathbf{d}} & \frac{\partial \mathbf{H}_d}{\partial {}^{\mathcal{I}}\boldsymbol{\theta}} & \frac{\partial \mathbf{H}_d}{\partial {}^{\mathcal{I}}\mathbf{t}_{\mathcal{B}}^{\mathcal{I}}} \end{bmatrix}, \quad (23)$$

where,

$$\begin{aligned} \frac{\partial \mathbf{H}_d}{\partial \mathbf{v}_k} &= -\frac{U_s}{m} {}^{\mathcal{I}}\mathbf{R} D_{\mathcal{B}}^{\mathcal{G}} \mathbf{R}^{\top}, \\ \frac{\partial \mathbf{H}_d}{\partial \tau} &= \frac{U_s}{m} {}^{\mathcal{I}}\mathbf{r}_3, \\ \frac{\partial \mathbf{H}_d}{\partial \mathbf{d}} &= -\frac{U_s}{m} [{}^{\mathcal{I}}\mathbf{r}_1^{\mathcal{G}} \mathbf{r}_1^{\top \mathcal{G}} \mathbf{v}_{\mathcal{B}}^{\mathcal{G}} \quad {}^{\mathcal{I}}\mathbf{r}_2^{\mathcal{G}} \mathbf{r}_2^{\top \mathcal{G}} \mathbf{v}_{\mathcal{B}}^{\mathcal{G}} \quad {}^{\mathcal{I}}\mathbf{r}_3^{\mathcal{G}} \mathbf{r}_3^{\top \mathcal{G}} \mathbf{v}_{\mathcal{B}}^{\mathcal{G}}], \\ \frac{\partial \mathbf{H}_d}{\partial {}^{\mathcal{I}}\boldsymbol{\theta}} &= \frac{1}{m} {}^{\mathcal{I}}\mathbf{R} \left(-\tau U_{ss} [\mathbf{e}_3]_{\times} + U_s \left([D_{\mathcal{B}}^{\mathcal{G}} \mathbf{R}^{\top \mathcal{G}} \mathbf{v}_{\mathcal{B}}^{\mathcal{G}}]_{\times} - D [{}^{\mathcal{G}}\mathbf{R}^{\top \mathcal{G}} \mathbf{v}_{\mathcal{B}}^{\mathcal{G}}]_{\times} \right) - [\hat{\mathbf{f}}_{res}]_{\times} \right), \\ \frac{\partial \mathbf{H}_d}{\partial {}^{\mathcal{I}}\mathbf{t}_{\mathcal{B}}^{\mathcal{I}}} &= [{}^{\mathcal{I}}\hat{\boldsymbol{\omega}}]_{\times} [{}^{\mathcal{I}}\hat{\boldsymbol{\omega}}]_{\times} + [{}^{\mathcal{I}}\hat{\boldsymbol{\alpha}}]_{\times}. \end{aligned} \quad (24)$$

Specifically, ${}^{\mathcal{I}}\hat{\boldsymbol{\alpha}}$ is the angular acceleration in the \mathcal{I} frame, which is obtained by differentiating the angular velocity, ${}^{\mathcal{I}}\hat{\boldsymbol{\alpha}} = \frac{d}{dt} {}^{\mathcal{I}}\hat{\boldsymbol{\omega}}$. In practice, we low-pass filter the $\hat{\boldsymbol{\omega}}, \hat{\boldsymbol{\alpha}}$ to reduce noise. And, the noise of IMU acceleration measurements is $\mathbf{n}_a \sim \mathcal{N}(0, \Sigma_a^2)$.

b) *network velocity measurements*: The velocity measurements from *V-P Net* are expressed as:

$$\begin{aligned} \hat{\mathbf{v}} &= \mathbf{H}_v(\mathbf{x}, \mathbf{n}_v) \\ &= {}^{\mathcal{G}}\mathbf{v}_{\mathcal{B}}^{\mathcal{G}} - {}^{\mathcal{G}}\mathbf{R} ({}^{\mathcal{I}}\hat{\boldsymbol{\omega}} \times {}^{\mathcal{I}}\mathbf{t}_{\mathcal{B}}^{\mathcal{I}}) + \mathbf{n}_v, \end{aligned} \quad (25)$$

whose jacobian can be given as:

$$\frac{\partial \mathbf{H}_v}{\partial \mathbf{x}_k} = \begin{bmatrix} \mathbf{0}_3 & \mathbf{I}_3 & \mathbf{0}_{31} & \mathbf{0}_3 & \mathbf{0}_3 & \frac{\partial \mathbf{r}_v}{\partial {}^{\mathcal{I}}\mathbf{t}_{\mathcal{B}}^{\mathcal{I}}} \end{bmatrix}, \quad (26)$$

where,

$$\frac{\partial \mathbf{r}_v}{\partial {}^{\mathcal{I}}\mathbf{t}_{\mathcal{B}}^{\mathcal{I}}} = -{}^{\mathcal{G}}\mathbf{R} [{}^{\mathcal{I}}\hat{\boldsymbol{\omega}}]_{\times}. \quad (27)$$

Specifically, the noise of network velocity measurements is $\mathbf{n}_v \sim \mathcal{N}(0, \hat{\Sigma}_v^2)$.

c) *network displacement measurements*: The displacement measurements from *V-P Net* are expressed as:

$$\begin{aligned} \hat{\mathbf{p}} &= \mathbf{H}_p(\mathbf{x}, \mathbf{n}_p) \\ &= {}^{\mathcal{G}}\mathbf{p}_{\mathcal{B}}^{\mathcal{G}} - {}^{\mathcal{G}}\mathbf{R} {}^{\mathcal{I}}\mathbf{t}_{\mathcal{B}}^{\mathcal{I}} + \mathbf{n}_p, \end{aligned} \quad (28)$$

whose jacobian can be given as:

$$\frac{\partial \mathbf{H}_p}{\partial \mathbf{x}_k} = \begin{bmatrix} \mathbf{I}_3 & \mathbf{0}_3 & \mathbf{0}_{31} & \mathbf{0}_3 & \mathbf{0}_3 & \frac{\partial \mathbf{H}_p}{\partial {}^{\mathcal{I}}\mathbf{t}_{\mathcal{B}}^{\mathcal{I}}} \end{bmatrix}, \quad (29)$$

where,

$$\frac{\partial \mathbf{H}_p}{\partial {}^{\mathcal{I}}\mathbf{t}_{\mathcal{B}}^{\mathcal{I}}} = -{}^{\mathcal{G}}\mathbf{R}. \quad (30)$$

Specifically, the noise of network displacement measurements is $\mathbf{n}_p \sim \mathcal{N}(0, \hat{\Sigma}_p^2)$.

4) *Discrete Extended Kalman Filter*: The complete EKF procedures for both rotation and translation can be written in a discretized form as follows:

$$\begin{aligned}
\mathbf{x}_{k+1|k} &= \mathbf{F}(\mathbf{x}_{k|k}, \mathbf{u}_k), \\
\mathbf{P}_{k+1|k} &= \mathbf{F}_x \mathbf{P}_{k|k} \mathbf{F}_x^T + \mathbf{F}_u \mathbf{Q}_k \mathbf{F}_u^T, \\
\mathbf{K}_{k+1} &= \mathbf{P}_{k+1|k} \mathbf{H}_x^T \left(\mathbf{H}_x \mathbf{P}_{k+1|k} \mathbf{H}_x^T + \mathbf{R}_{k+1} \right)^{-1}, \\
\mathbf{x}_{k+1|k+1} &= \mathbf{x}_{k+1|k} \oplus \left(\mathbf{K}_{k+1} (\mathbf{z}_{k+1} - h(\mathbf{x}_{k+1|k})) \right), \\
\mathbf{P}_{k+1|k+1} &= (\mathbf{I} - \mathbf{K}_{k+1} \mathbf{H}_x) \mathbf{P}_{k+1|k},
\end{aligned} \tag{31}$$

where,

$$\mathbf{Q} = \widehat{\Sigma}_f^2, \quad \mathbf{R} = \text{diag}\{\Sigma_a^2, \widehat{\Sigma}_v^2, \widehat{\Sigma}_p^2\}. \tag{32}$$

III. ONE-STAGE EKF FOR INERTIAL DYNAMICAL FUSION

A. State

The state of the system is defined as:

$$\mathbf{x} = (\mathcal{G} \mathbf{q}, \mathcal{G} \mathbf{p}_{\mathcal{B}}^{\mathcal{G}}, \mathcal{G} \mathbf{v}_{\mathcal{B}}^{\mathcal{G}}, \tau, \mathbf{d}, \mathcal{I}_{\mathcal{B}} \mathbf{q}, \mathcal{I}_{\mathcal{B}} \mathbf{t}_{\mathcal{B}}^{\mathcal{I}}). \tag{33}$$

B. Process Model

We regard the quadrotor dynamics and gyroscope outputs of *De-Bias Net* as the input, and express the complete process model as follows:

$$\begin{aligned}
\mathcal{G} \dot{\mathbf{q}} &= \frac{1}{2} \mathcal{G} \mathbf{q} \otimes (\mathcal{I} \widehat{\boldsymbol{\omega}} + \mathbf{n}_{\omega}), \\
\mathcal{G} \dot{\mathbf{p}}_{\mathcal{B}}^{\mathcal{G}} &= \mathcal{G} \mathbf{v}_{\mathcal{B}}^{\mathcal{G}}, \\
\mathcal{G} \dot{\mathbf{v}}_{\mathcal{B}}^{\mathcal{G}} &= \frac{1}{m} \mathcal{G} \mathbf{R} \left(\tau U_{ss} \mathbf{e}_3 - U_s D_{\mathcal{B}}^{\mathcal{G}} \mathbf{R}^{\top} \mathcal{G} \mathbf{v}_{\mathcal{B}}^{\mathcal{G}} + \widehat{\mathbf{f}}_{res} + \mathcal{G} \mathbf{n}_f \right) - \mathcal{G} \mathbf{g}, \\
\dot{\tau} &= 0, \\
\dot{\mathbf{d}} &= 0, \\
\mathcal{I}_{\mathcal{B}} \dot{\mathbf{q}} &= 0, \\
\mathcal{I}_{\mathcal{B}} \dot{\mathbf{t}}_{\mathcal{B}}^{\mathcal{I}} &= 0,
\end{aligned} \tag{34}$$

The above differential equation is discretized as follows:

$$\begin{aligned}
\mathbf{x}_{k+1} &= \mathbf{F}(\mathbf{x}_k, \mathbf{u}_k) \\
&= \mathbf{F}_x \mathbf{x}_k + \mathbf{F}_n \mathbf{n}_k,
\end{aligned} \tag{35}$$

where,

$$\begin{aligned}
\mathbf{F}_x &= \begin{bmatrix} \frac{\partial \mathcal{G} \boldsymbol{\theta}_{k+1}}{\partial \mathcal{G} \boldsymbol{\theta}_k} & \mathbf{0}_3 & \mathbf{0}_3 & \mathbf{0}_{31} & \mathbf{0}_3 & \mathbf{0}_3 & \mathbf{0}_3 \\ \mathbf{0}_3 & \mathbf{I}_3 & \mathbf{I}_3 \Delta t & \mathbf{0}_{31} & \mathbf{0}_3 & \mathbf{0}_3 & \mathbf{0}_3 \\ \frac{\partial \mathbf{v}_{k+1}}{\partial \mathcal{G} \boldsymbol{\theta}_k} & \mathbf{0}_3 & \frac{\partial \mathbf{v}_{k+1}}{\partial \mathbf{v}_k} & \frac{\partial \mathbf{v}_{k+1}}{\partial \tau} & \frac{\partial \mathbf{v}_{k+1}}{\partial \mathbf{d}} & \frac{\partial \mathbf{v}_{k+1}}{\partial \mathcal{I}_{\mathcal{B}} \boldsymbol{\theta}} & \mathbf{0}_3 \\ \mathbf{0}_3 & \mathbf{0}_{13} & \mathbf{0}_{13} & 1 & \mathbf{0}_{13} & \mathbf{0}_{13} & \mathbf{0}_{13} \\ \mathbf{0}_3 & \mathbf{0}_3 & \mathbf{0}_3 & \mathbf{0}_{31} & \mathbf{I}_3 & \mathbf{0}_3 & \mathbf{0}_3 \\ \mathbf{0}_3 & \mathbf{0}_3 & \mathbf{0}_3 & \mathbf{0}_{31} & \mathbf{0}_3 & \mathbf{I}_3 & \mathbf{0}_3 \\ \mathbf{0}_3 & \mathbf{0}_3 & \mathbf{0}_3 & \mathbf{0}_{31} & \mathbf{0}_3 & \mathbf{0}_3 & \mathbf{I}_3 \end{bmatrix}, \\
\mathbf{F}_n &= \begin{bmatrix} \frac{\partial \mathcal{G} \boldsymbol{\theta}_{k+1}}{\partial \mathbf{n}_{\omega}} & \mathbf{0}_3 & \mathbf{0}_3 & \mathbf{0}_{31} & \mathbf{0}_3 & \mathbf{0}_3 \\ \mathbf{0}_3 & \mathbf{0}_3 & \frac{\partial \mathbf{v}_{k+1}}{\partial \mathbf{n}_f} & \mathbf{0}_{31} & \mathbf{0}_3 & \mathbf{0}_3 \end{bmatrix}^{\top}.
\end{aligned} \tag{36}$$

Specifically,

$$\begin{aligned}
\frac{\partial_{\mathcal{I}}^{\mathcal{G}} \boldsymbol{\theta}_{k+1}}{\partial_{\mathcal{I}}^{\mathcal{G}} \boldsymbol{\theta}_k} &= \text{Exp}(-{}^{\mathcal{I}}\hat{\boldsymbol{\omega}} \Delta t), \\
\frac{\partial \mathbf{v}_{k+1}}{\partial_{\mathcal{I}}^{\mathcal{G}} \boldsymbol{\theta}_k} &= \frac{\Delta t}{m} {}^{\mathcal{I}}\mathbf{R} \left(-\tau U_{ss} [{}^{\mathcal{I}}_{\mathcal{B}} \mathbf{r}_3]_{\times} + U_s \left({}^{\mathcal{G}}\mathbf{R} [{}^{\mathcal{I}}_{\mathcal{B}} \mathbf{R} D_{\mathcal{B}}^{\mathcal{G}} \mathbf{R}^{\top \mathcal{G}} \mathbf{v}_{\mathcal{B}}^{\mathcal{G}}]_{\times} - {}^{\mathcal{G}}\mathbf{R} D_{\mathcal{B}}^{\mathcal{I}} \mathbf{R}^{\top} [{}^{\mathcal{G}}\mathbf{R}^{\top \mathcal{G}} \mathbf{v}_{\mathcal{B}}^{\mathcal{G}}]_{\times} \right) - [{}^{\mathcal{I}}_{\mathcal{B}} \mathbf{R} \hat{\mathbf{f}}_{res}]_{\times} \right), \\
\frac{\partial \mathbf{v}_{k+1}}{\partial \mathbf{v}_k} &= \mathbf{I} - \frac{U_s \Delta t}{m} {}^{\mathcal{G}}_{\mathcal{B}} \mathbf{R} D_{\mathcal{B}}^{\mathcal{G}} \mathbf{R}^{\top}, \\
\frac{\partial \mathbf{v}_{k+1}}{\partial \tau} &= \frac{U_{ss} \Delta t}{m} {}^{\mathcal{G}}_{\mathcal{B}} \mathbf{r}_3, \\
\frac{\partial \mathbf{v}_{k+1}}{\partial \mathbf{d}} &= -\frac{\Delta t}{m} [{}^{\mathcal{G}}_{\mathcal{B}} \mathbf{r}_1 {}^{\mathcal{G}}_{\mathcal{B}} \mathbf{r}_1^{\top \mathcal{G}} \mathbf{v}_{\mathcal{B}}^{\mathcal{G}} \quad {}^{\mathcal{G}}_{\mathcal{B}} \mathbf{r}_2 {}^{\mathcal{G}}_{\mathcal{B}} \mathbf{r}_2^{\top \mathcal{G}} \mathbf{v}_{\mathcal{B}}^{\mathcal{G}} \quad {}^{\mathcal{G}}_{\mathcal{B}} \mathbf{r}_3 {}^{\mathcal{G}}_{\mathcal{B}} \mathbf{r}_3^{\top \mathcal{G}} \mathbf{v}_{\mathcal{B}}^{\mathcal{G}}], \\
\frac{\partial \mathbf{v}_{k+1}}{\partial {}^{\mathcal{I}}\boldsymbol{\theta}} &= \frac{\Delta t}{m} {}^{\mathcal{G}}_{\mathcal{B}} \mathbf{R} \left(-\tau U_{ss} [\mathbf{e}_3]_{\times} + U_s \left([D_{\mathcal{B}}^{\mathcal{G}} \mathbf{R}^{\top \mathcal{G}} \mathbf{v}_{\mathcal{B}}^{\mathcal{G}}]_{\times} - D [{}^{\mathcal{G}}_{\mathcal{B}} \mathbf{R}^{\top \mathcal{G}} \mathbf{v}_{\mathcal{B}}^{\mathcal{G}}]_{\times} \right) - [\hat{\mathbf{f}}_{res}]_{\times} \right), \\
\frac{\partial_{\mathcal{I}}^{\mathcal{G}} \boldsymbol{\theta}_{k+1}}{\partial \mathbf{n}_{\omega}} &= \mathbf{J}_r({}^{\mathcal{I}}\hat{\boldsymbol{\omega}} \Delta t) \Delta t, \\
\frac{\partial \mathbf{v}_{k+1}}{\partial \mathbf{n}_f} &= \frac{1}{m} {}^{\mathcal{G}}_{\mathcal{B}} \mathbf{R} \Delta t,
\end{aligned} \tag{37}$$

where,

$$\mathbf{J}_r(\boldsymbol{\theta}) = \mathbf{I}_3 - \frac{1 - \cos||\boldsymbol{\theta}||}{||\boldsymbol{\theta}||^2} [\boldsymbol{\theta}]_{\times} + \frac{||\boldsymbol{\theta}|| - \sin||\boldsymbol{\theta}||}{||\boldsymbol{\theta}||^3} [\boldsymbol{\theta}]_{\times}^2 \tag{38}$$

C. Measurement Model

1) *gravity alignment measurements*: The attitude controllers of most flying robots rely on the complementary filters [2, 3] to obtain attitude observations. Similarly, we consider the gravity alignment constraint to obtain the tilt observation:

$$\begin{aligned}
{}^{\mathcal{I}}\hat{\mathbf{a}} &= \mathbf{H}_g(\mathbf{x}, \mathbf{n}_g) \\
&\approx {}^{\mathcal{G}}_{\mathcal{I}} \mathbf{R}^{\top \mathcal{G}} \mathbf{g} + \mathbf{n}_g,
\end{aligned} \tag{39}$$

whose jacobian can be given as:

$$\frac{\partial \mathbf{H}_g}{\partial \mathbf{x}_k} = \left[\frac{\partial \mathbf{H}_g}{\partial_{\mathcal{I}}^{\mathcal{G}} \boldsymbol{\theta}_k} \quad \mathbf{0}_3 \quad \mathbf{0}_3 \quad \mathbf{0}_{31} \quad \mathbf{0}_3 \quad \mathbf{0}_3 \quad \mathbf{0}_3 \right], \tag{40}$$

where,

$$\frac{\partial \mathbf{H}_g}{\partial_{\mathcal{I}}^{\mathcal{G}} \boldsymbol{\theta}_k} = [{}^{\mathcal{G}}_{\mathcal{I}} \mathbf{R}^{\top \mathcal{G}} \mathbf{g}]_{\times}. \tag{41}$$

2) *dynamics constraint measurements*: The dynamics constraint measurements are expressed as:

$$\begin{aligned}
{}^{\mathcal{I}}\hat{\mathbf{a}} &= \mathbf{H}_d(\mathbf{x}, \mathbf{n}_a) \\
&= \frac{1}{m} {}^{\mathcal{I}}_{\mathcal{B}} \mathbf{R} \left(\tau U_{ss} \mathbf{e}_3 - U_s D_{\mathcal{B}}^{\mathcal{G}} \mathbf{R}^{\top \mathcal{G}} \mathbf{v}_{\mathcal{B}}^{\mathcal{G}} + \hat{\mathbf{f}}_{res} \right) + {}^{\mathcal{I}}\hat{\boldsymbol{\omega}} \times ({}^{\mathcal{I}}\hat{\boldsymbol{\omega}} \times {}^{\mathcal{I}}\mathbf{t}_{\mathcal{B}}^{\mathcal{I}}) + {}^{\mathcal{I}}\hat{\boldsymbol{\alpha}} \times {}^{\mathcal{I}}\mathbf{t}_{\mathcal{B}}^{\mathcal{I}} + \mathbf{n}_a,
\end{aligned} \tag{42}$$

whose jacobian can be given as:

$$\frac{\partial \mathbf{H}_d}{\partial \mathbf{x}_k} = \left[\frac{\partial \mathbf{H}_d}{\partial_{\mathcal{I}}^{\mathcal{G}} \boldsymbol{\theta}_k} \quad \mathbf{0}_3 \quad \frac{\partial \mathbf{H}_d}{\partial \mathbf{v}_k} \quad \frac{\partial \mathbf{H}_d}{\partial \tau} \quad \frac{\partial \mathbf{H}_d}{\partial \mathbf{d}} \quad \frac{\partial \mathbf{H}_d}{\partial {}^{\mathcal{I}}\boldsymbol{\theta}} \quad \frac{\partial \mathbf{H}_d}{\partial {}^{\mathcal{I}}\mathbf{t}_{\mathcal{B}}^{\mathcal{I}}} \right], \tag{43}$$

where,

$$\begin{aligned}
\frac{\partial \mathbf{H}_d}{\partial \mathcal{I}\boldsymbol{\theta}_k} &= -\frac{U_s}{m} \mathbf{R} D_{\mathcal{B}}^{\mathcal{I}} \mathbf{R}^{\top} \left[\mathcal{I}^{\mathcal{G}} \mathbf{R}^{\top \mathcal{G}} \mathbf{v}_{\mathcal{B}}^{\mathcal{G}} \right]_{\times}, \\
\frac{\partial \mathbf{H}_d}{\partial \mathbf{v}_k} &= -\frac{U_s}{m} \mathbf{R} D_{\mathcal{B}}^{\mathcal{G}} \mathbf{R}^{\top}, \\
\frac{\partial \mathbf{H}_d}{\partial \tau} &= \frac{U_s}{m} \mathbf{r}_3, \\
\frac{\partial \mathbf{H}_d}{\partial \mathbf{d}} &= -\frac{U_s}{m} \left[\mathcal{B}^{\mathcal{I}} \mathbf{r}_1^{\mathcal{G}} \mathbf{r}_1^{\top \mathcal{G}} \mathbf{v}_{\mathcal{B}}^{\mathcal{G}} \quad \mathcal{B}^{\mathcal{I}} \mathbf{r}_2^{\mathcal{G}} \mathbf{r}_2^{\top \mathcal{G}} \mathbf{v}_{\mathcal{B}}^{\mathcal{G}} \quad \mathcal{B}^{\mathcal{I}} \mathbf{r}_3^{\mathcal{G}} \mathbf{r}_3^{\top \mathcal{G}} \mathbf{v}_{\mathcal{B}}^{\mathcal{G}} \right], \\
\frac{\partial \mathbf{H}_d}{\partial \mathcal{I}\boldsymbol{\theta}} &= \frac{1}{m} \mathcal{B}^{\mathcal{I}} \mathbf{R} \left(-k U_{ss} \left[\mathbf{e}_3 \right]_{\times} + U_s \left(\left[D_{\mathcal{B}}^{\mathcal{G}} \mathbf{R}^{\top \mathcal{G}} \mathbf{v}_{\mathcal{B}}^{\mathcal{G}} \right]_{\times} - D \left[\mathcal{B}^{\mathcal{G}} \mathbf{R}^{\top \mathcal{G}} \mathbf{v}_{\mathcal{B}}^{\mathcal{G}} \right]_{\times} \right) - \left[\hat{\mathbf{f}}_{res} \right]_{\times} \right), \\
\frac{\partial \mathbf{H}_d}{\partial \mathcal{I}\mathbf{t}_{\mathcal{B}}^{\mathcal{I}}} &= \left[\mathcal{I}^{\widehat{\boldsymbol{\omega}}} \right]_{\times} \left[\mathcal{I}^{\widehat{\boldsymbol{\omega}}} \right]_{\times} + \left[\mathcal{I}^{\widehat{\boldsymbol{\alpha}}} \right]_{\times}.
\end{aligned} \tag{44}$$

Specifically, $\mathcal{I}^{\widehat{\boldsymbol{\alpha}}}$ is the angular acceleration in the \mathcal{I} frame, which is obtained by differentiating the angular velocity, $\mathcal{I}^{\widehat{\boldsymbol{\alpha}}} = \frac{d}{dt} \mathcal{I}^{\widehat{\boldsymbol{\omega}}}$. In practice, we low-pass filter the $\widehat{\boldsymbol{\omega}}, \widehat{\boldsymbol{\alpha}}$ to reduce noise. And, the noise of IMU acceleration measurements is $\mathbf{n}_a \sim \mathcal{N}(0, \Sigma_a^2)$.

3) *network velocity measurements*: The velocity measurements from *V-P Net* are expressed as:

$$\begin{aligned}
\hat{\mathbf{v}} &= \mathbf{H}_v(\mathbf{x}, \mathbf{n}_v) \\
&= \mathcal{G} \mathbf{v}_{\mathcal{B}}^{\mathcal{G}} - \mathcal{I}^{\mathcal{G}} \mathbf{R} \left(\mathcal{I}^{\widehat{\boldsymbol{\omega}}} \times \mathcal{I}\mathbf{t}_{\mathcal{B}}^{\mathcal{I}} \right) + \mathbf{n}_v,
\end{aligned} \tag{45}$$

whose jacobian can be given as:

$$\frac{\partial \mathbf{H}_v}{\partial \mathbf{x}_k} = \begin{bmatrix} \frac{\partial \mathbf{H}_v}{\partial \mathcal{I}\boldsymbol{\theta}_k} & \mathbf{0}_3 & \mathbf{I}_3 & \mathbf{0}_{31} & \mathbf{0}_3 & \mathbf{0}_3 & \frac{\partial \mathbf{H}_v}{\partial \mathcal{I}\mathbf{t}_{\mathcal{B}}^{\mathcal{I}}} \end{bmatrix}, \tag{46}$$

where,

$$\begin{aligned}
\frac{\partial \mathbf{H}_v}{\partial \mathcal{I}\boldsymbol{\theta}_k} &= \mathcal{I}^{\mathcal{G}} \mathbf{R} \left[\mathcal{I}^{\widehat{\boldsymbol{\omega}}} \times \mathcal{I}\mathbf{t}_{\mathcal{B}}^{\mathcal{I}} \right]_{\times}, \\
\frac{\partial \mathbf{H}_v}{\partial \mathcal{I}\mathbf{t}_{\mathcal{B}}^{\mathcal{I}}} &= -\mathcal{I}^{\mathcal{G}} \mathbf{R} \left[\mathcal{I}^{\widehat{\boldsymbol{\omega}}} \right]_{\times}.
\end{aligned} \tag{47}$$

Specifically, the noise of network velocity measurements is $\mathbf{n}_v \sim \mathcal{N}(0, \hat{\Sigma}_v^2)$.

4) *network displacement measurements*: The displacement measurements from *V-P Net* are expressed as:

$$\begin{aligned}
\hat{\mathbf{p}} &= \mathbf{H}_p(\mathbf{x}, \mathbf{n}_p) \\
&= \mathcal{G} \mathbf{p}_{\mathcal{B}}^{\mathcal{G}} - \mathcal{I}^{\mathcal{G}} \mathbf{R}^{\mathcal{I}} \mathbf{t}_{\mathcal{B}}^{\mathcal{I}} + \mathbf{n}_p,
\end{aligned} \tag{48}$$

whose jacobian can be given as:

$$\frac{\partial \mathbf{H}_p}{\partial \mathbf{x}_k} = \begin{bmatrix} \frac{\partial \mathbf{H}_p}{\partial \mathcal{I}\boldsymbol{\theta}_k} & \mathbf{I}_3 & \mathbf{0}_3 & \mathbf{0}_{31} & \mathbf{0}_3 & \mathbf{0}_3 & \frac{\partial \mathbf{H}_p}{\partial \mathcal{I}\mathbf{t}_{\mathcal{B}}^{\mathcal{I}}} \end{bmatrix}, \tag{49}$$

where,

$$\begin{aligned}
\frac{\partial \mathbf{H}_p}{\partial \mathcal{I}\boldsymbol{\theta}_k} &= \mathcal{I}^{\mathcal{G}} \mathbf{R} \left[\mathcal{I}\mathbf{t}_{\mathcal{B}}^{\mathcal{I}} \right]_{\times}, \\
\frac{\partial \mathbf{H}_p}{\partial \mathcal{I}\mathbf{t}_{\mathcal{B}}^{\mathcal{I}}} &= -\mathcal{I}^{\mathcal{G}} \mathbf{R}.
\end{aligned} \tag{50}$$

Specifically, the noise of network displacement measurements is $\mathbf{n}_p \sim \mathcal{N}(0, \hat{\Sigma}_p^2)$.

D. Discrete Extended Kalman Filter

The complete EKF procedures for both rotation and translation can be written in a discretized form as follows:

$$\begin{aligned}\mathbf{x}_{k+1|k} &= \mathbf{F}(\mathbf{x}_{k|k}, \mathbf{u}_k), \\ \mathbf{P}_{k+1|k} &= \mathbf{F}_x \mathbf{P}_{k|k} \mathbf{F}_x^T + \mathbf{F}_u \mathbf{Q}_k \mathbf{F}_u^T, \\ \mathbf{K}_{k+1} &= \mathbf{P}_{k+1|k} \mathbf{H}_x^T (\mathbf{H}_x \mathbf{P}_{k+1|k} \mathbf{H}_x^T + \mathbf{R}_{k+1})^{-1}, \\ \mathbf{x}_{k+1|k+1} &= \mathbf{x}_{k+1|k} \oplus (\mathbf{K}_{k+1} (\mathbf{z}_{k+1} - h(\mathbf{x}_{k+1|k}))), \\ \mathbf{P}_{k+1|k+1} &= (\mathbf{I} - \mathbf{K}_{k+1} \mathbf{H}_x) \mathbf{P}_{k+1|k}.\end{aligned}\quad (51)$$

where,

$$\mathbf{Q} = \text{diag}\{\Sigma_\omega^2, \hat{\Sigma}_f^2\}, \quad \mathbf{R} = \text{diag}\{\Sigma_a^2, \hat{\Sigma}_v^2, \hat{\Sigma}_p^2\}. \quad (52)$$

IV. OBSERVABILITY ANALYSIS

According to the observability analysis method developed in [4], we could analyze the observability of a control affine system by checking the observability rank criterion.

For the rotation stage which is driven by Eq. (9) and observed by Eq. (12), the rotation ${}^G\mathbf{q}$ is composed of two observable angles (roll and pitch) and an unobservable yaw angle.

For the translation stage, we firstly write the process model of the system in control affine form:

$$\dot{\mathbf{x}} = \mathbf{f}_0(\mathbf{x}) + \sum_{i=1}^n \mathbf{f}_i(\mathbf{x}) \mathbf{u}_i. \quad (53)$$

Since the four motor speeds of the quadrotor are integrated into the two inputs U_{ss} and U_s in Eq. (18), our system could be presented:

$$\begin{aligned}\dot{\mathbf{x}} &= \mathbf{f}_0(\mathbf{x}) + \mathbf{f}_1(\mathbf{x}) U_{ss} + \mathbf{f}_2(\mathbf{x}) U_s \\ &= \begin{bmatrix} {}^G\mathbf{v}_B^G \\ -{}^G\mathbf{g} \\ \mathbf{0}_{10 \times 1} \end{bmatrix} + \begin{bmatrix} \mathbf{0}_{3 \times 1} \\ \frac{1}{m} {}^G\mathbf{R} \tau \mathbf{e}_3 \\ \mathbf{0}_{10 \times 1} \end{bmatrix} U_{ss} + \begin{bmatrix} \mathbf{0}_{3 \times 1} \\ -\frac{1}{m} {}^G\mathbf{R} D_B^G \mathbf{R}^\top {}^G\mathbf{v}_B^G \\ \mathbf{0}_{10 \times 1} \end{bmatrix} U_s.\end{aligned}\quad (54)$$

And then, we simplify the three measurement models Eq. (22, 25, 28) as:

$$\begin{aligned}\mathbf{h}_d &= \frac{1}{m} {}^G\mathbf{R} (\tau U_{ss} \mathbf{e}_3 - U_s D_B^G \mathbf{R}^\top {}^G\mathbf{v}_B^G) + {}^I\hat{\omega} \times ({}^I\hat{\omega} \times {}^I\mathbf{t}_B^I) + {}^I\hat{\alpha} \times {}^I\mathbf{t}_B^I, \\ \mathbf{h}_v &= {}^G\mathbf{v}_B^G - {}^G\mathbf{R} ({}^I\hat{\omega} \times {}^I\mathbf{t}_B^I), \\ \mathbf{h}_p &= {}^G\mathbf{p}_B^G - {}^G\mathbf{R} {}^I\mathbf{t}_B^I.\end{aligned}\quad (55)$$

We use Lie derivatives to quantify the impact of changes in the control input U_{ss} and U_s on the output functions \mathbf{h}_d , \mathbf{h}_v and \mathbf{h}_p .

$$\begin{aligned}L^0 \mathbf{h} &= \mathbf{h}, \\ L_{\mathbf{f}_{i_1}, \mathbf{f}_{i_2}, \dots, \mathbf{f}_{i_{k+1}}}^{k+1} \mathbf{h} &= \nabla_{\mathbf{x}} \left(L_{\mathbf{f}_{i_1}, \mathbf{f}_{i_2}, \dots, \mathbf{f}_{i_k}}^k \mathbf{h} \right) \mathbf{f}_{i_{k+1}}\end{aligned}\quad (56)$$

We stack vertically several Lie derivatives of the unforced vector field \mathbf{f}_0 and the control input vector fields \mathbf{f}_1 and \mathbf{f}_2 into a vector \mathcal{O} :

$$\mathcal{O} = \begin{bmatrix} \mathbf{h}_d \\ \mathbf{h}_v \\ \mathbf{h}_p \\ L_{\mathbf{f}_0} \mathbf{h}_d \\ L_{\mathbf{f}_0} \mathbf{h}_p \\ L_{\mathbf{f}_1} \mathbf{h}_d \\ L_{\mathbf{f}_1} \mathbf{h}_v \\ L_{\mathbf{f}_2} \mathbf{h}_v \end{bmatrix}, \quad (57)$$

and calculate its gradients as observability matrix $\nabla_x \mathcal{O}$. Finally, we can evaluate whether the system is locally observable by checking the observability rank criterion. In general, the rank is:

$$\text{rank}\{\nabla_x \mathcal{O}\} = 11. \quad (58)$$

However, under some certain conditions the matrix has a rank deficiency. Some of these cases are when:

$$\begin{cases} {}^{\mathcal{I}}\hat{\omega} = \mathbf{0}_{3 \times 1}, {}^{\mathcal{I}}\mathbf{t}_{\mathcal{B}}^{\mathcal{T}} \text{ is unobservable;} \\ {}^g\mathbf{v}_{\mathcal{B}}^g = \mathbf{0}_{3 \times 1}, D \text{ and } {}^{\mathcal{I}}\mathbf{R} \text{ are unobservable;} \\ {}^g\mathbf{v}_{\mathcal{B}}^g = [0; 0; *], \text{yaw}({}^{\mathcal{I}}\mathbf{R}) \text{ is unobservable,} \end{cases} \quad (59)$$

which means the corresponding parameters to be estimated may not converge under the above conditions.

V. ONE-STAGE OR TWO-STAGE

In the one-stage EKF, all Eq. (42), Eq. (45) and Eq. (48) will update the ${}^g\mathbf{q}$. To demonstrate the effect of these three measurement models on the state estimation system, we design four experiments, namely, with *ad* update, *vd* update, *pd* update and *pvad* update. As shown in the Fig. 1, rotation is prone to be incorrectly updated by each noisy observation in the one-stage EKF, which further affects the estimation of velocity and position. This is due to the fact that rotation is very sensitive as an explicit or implicit input to the networks. Once the rotation can not be updated correctly during the EKF process, it will make the outputs of networks worse and thus affect the system state estimation.

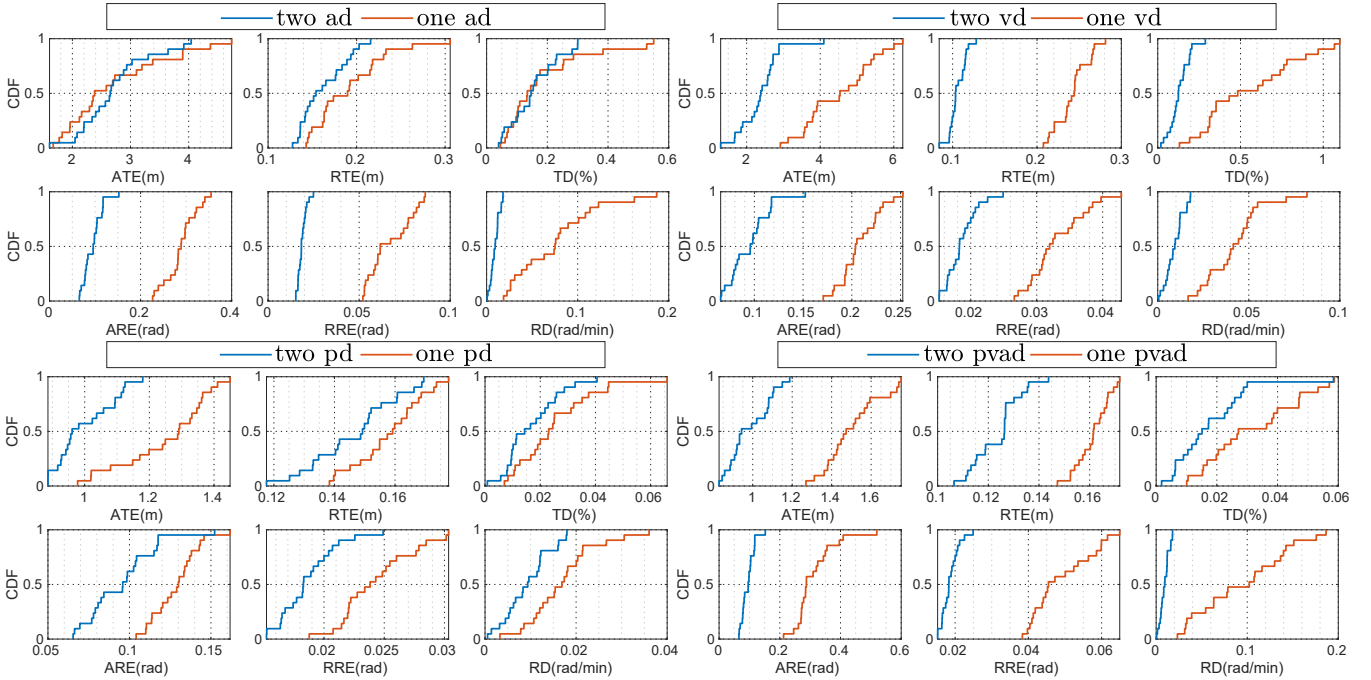


Fig. 1: Comparison of one-stage and two-stage EKF. *p,v,a* mean using position, velocity and acceleration to update, respectively, and *d* means using the *Res-Dynamics Net*. *one* and *two* means one-stage and two-stage EKF. Such as, *one ad* means one-stage EKF using acceleration to update and the *Res-Dynamics Net*.

REFERENCES

- [1] J. Svacha, J. Paulos, G. Loianno, and V. Kumar, “Imu-based inertia estimation for a quadrotor using newton-euler dynamics,” *IEEE Robotics and Automation Letters*, vol. 5, no. 3, pp. 3861–3867, 2020.
- [2] R. Mahony, T. Hamel, and J.-M. Pflimlin, “Nonlinear complementary filters on the special orthogonal group,” *IEEE Transactions on automatic control*, vol. 53, no. 5, pp. 1203–1218, 2008.
- [3] S. O. Madgwick, A. J. Harrison, and R. Vaidyanathan, “Estimation of imu and marg orientation using a gradient descent algorithm,” in *2011 IEEE international conference on rehabilitation robotics*. IEEE, 2011, pp. 1–7.
- [4] R. Hermann and A. Krener, “Nonlinear controllability and observability,” *IEEE Transactions on automatic control*, vol. 22, no. 5, pp. 728–740, 1977.